nature geoscience

LETTERS

PUBLISHED ONLINE: 28 SEPTEMBER 2015 | DOI: 10.1038/NGEO2537

Protracted development of bioturbation through the early Palaeozoic Era

Lidya G. Tarhan[1,2]*, Mary L. Droser[2], Noah J. Planavsky[1] and David T. Johnston[3]

Bioturbation, the physical and chemical mixing of sediment by burrowing animals, exerts an important control on the character of modern marine sediments and biogeochemical cycling[1–9]. Here we show that the mixing of sediments on marine shelves remained limited until at least the late Silurian, 120 million years after the Precambrian–Cambrian transition. We present ichnological, stratigraphic and taphonomic data from a range of lower Phanerozoic siliciclastic successions spanning four palaeocontinents. The protracted development of the sediment mixed layer is also consistent with sulphur data and global sulphur model simulations. The slow increase in the intensity of bioturbation in the sediment record suggests that evolutionary advances in sediment colonization outpaced advances in sediment mixing. We conclude that ecosystem restructuring caused by the onset of significant infaunal mobile deposit feeding ('bulldozing') occurred well after both the Cambrian Explosion and the Great Ordovician Biodiversification Event.

The modern seafloor and the majority of the Phanerozoic stratigraphic record are characterized by biogenically reworked, well-churned sediment[7–10]. In modern oceans the 'mixed layer,' the zone of sediment which has been homogenized and fluidized by the activity of bioturbating organisms, extends to a depth of ~10 cm below the sediment–water interface[4–9]. This extensive sediment mixing, which is responsible for heightened nutrient cycling and the deep and widespread oxidation of the sediment pile, shapes the ecological and biogeochemical character of the seafloor[1–3]. However, the geologic timing of the development of the mixed layer has not been well constrained[11]. Previous attempts to track the global development of sediment mixing (for example, ref. 12) have largely not employed a stratigraphically continuous, field-based and facies-controlled approach, have focused on infaunalization rather than mixed layer development or have lacked sufficient geographic or temporal coverage (see Supplementary Information). As a result, the influence of bioturbation on ecosystem structuring and the evolution of global biogeochemical cycling remains poorly quantified. Here we provide a new and stratigraphically constrained, global and multiproxy record of the early development of sediment mixing.

Bioturbation data were collected from lowermost Cambrian through upper Silurian heterolithic siliciclastic shallow marine successions worldwide (Supplementary Fig. 1). Siliciclastic sediment and strata represent the vast majority of the modern seafloor and the stratigraphic record (for example, ref. 13), and shallow marine settings are the site of the majority of marine biogeochemical cycling (80–90% organic matter remineralization[14]). Data were collected from 22 units (see Supplementary Information) determined, on the basis of facies, fauna and palaeogeographic reconstruction, to represent deposition under shallow oxygenated marine waters. Sedimentological, ichnological and taphonomic data were collected from >700 m of section, comprising >40,200 discrete beds, to determine the extent of biogenic sediment mixing typical of early Palaeozoic marine shelfal environments.

To track mixing intensity we evaluated the rock record according to six criteria: bedding thickness; depth of bioturbation; biogenic fabric disruption; fidelity of trace fossil preservation (that is, bioglyphic preservation); complexity of trace fossil assemblages and abundance of surficially produced physical sedimentary structures. Although these metrics are related, they each provide unique information concerning substrate consistency, infaunal behaviour and the extent of seafloor sediment mixing (see Methods and Supplementary Information). The resulting suite of Cambrian–Silurian data represents the most high-resolution, stratigraphically and sedimentologically constrained and spatially and temporally representative database for this time interval. Data were grouped into three chronological intervals: lower–middle Cambrian (~542–507 Myr ago (Ma)), Cambro-Ordovician (~500–458 Ma) and Ordovician–Silurian (~450–420 Ma).

Lower–middle Cambrian strata (Fig. 1a–d; see ref. 11 for further details) are characterized by thin coherent beds (mm- to cm-scale; mean sandstone bed thickness = 1.3 cm (Fig. 2)) and well-preserved conformable bed junctions, without evidence for significant exhumation (for example, scouring, rip-ups, truncated burrows). Trace fossils are abundant along bed bases and burrows are most commonly preserved as passively infilled casts rather than bed-penetrative intra-bed structures. 'Floating' mm-scale burrows, infilled by means of bypass sedimentation, are common. Maximum burrow depth is typically on the mm scale and, excepting piperock (see Supplementary Information), never exceeds 3 cm. Millimetre-scale tool marks are common and occur densely. Trace fossil preservation is of a very high fidelity; discrete shallowly emplaced and surficial traces are sharply preserved; bioglyphs such as scratch marks and appendage imprints occur frequently, even where assemblage density approaches the highest levels of bedding plane surface coverage (bedding plane bioturbation index[15] [BPBI] 4–5). However, in spite of the dense colonization of bedding planes, stratigraphic fabrics—that is, the extent of disruption of depositional fabrics by burrowing (measured by ichnofabric index [ii], with ii 1 denoting laminated and ii 6 completely homogenized[16])—are characterized by an almost complete lack of disruption. The most disrupted intervals are characterized by a maximum ii of 3, but these zones of disruption are commonly confined to very limited spatial scales (mm to cm); average sample- and bed-scale ichnofabrics rarely exceed ii 2 (sample-averaged mean ii = 2.1;

[1]Department of Geology and Geophysics, Yale University, 210 Whitney Ave, New Haven, Connecticut 06511, USA. [2]Department of Earth Sciences, University of California-Riverside, 900 University Ave, Riverside, California 92521, USA. [3]Department of Earth and Planetary Sciences, Harvard University, 20 Oxford St., Cambridge, Massachusetts 02138, USA. *e-mail: lidya.tarhan@yale.edu

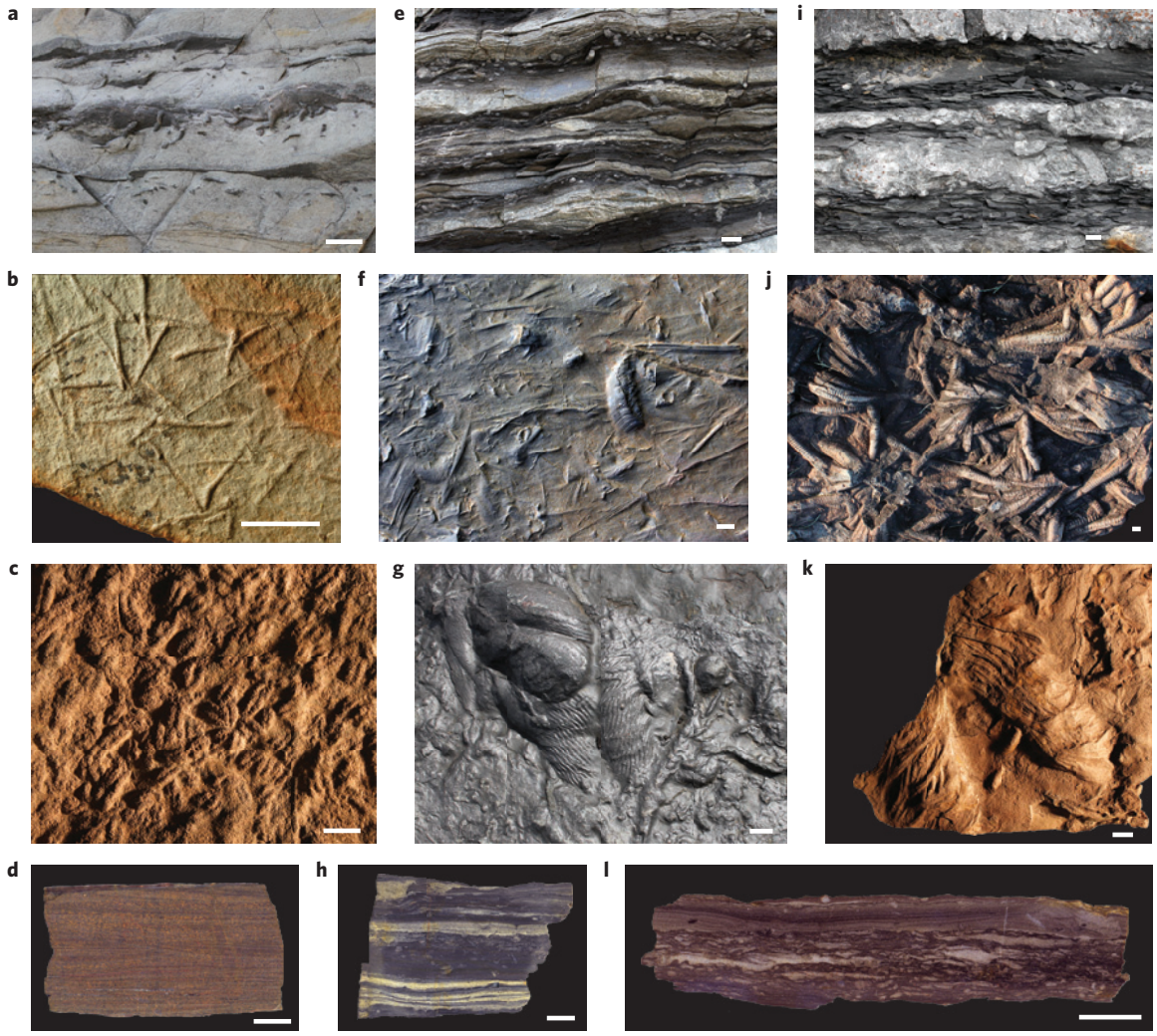

Figure 1 | Lower Palaeozoic trace fossil preservation and ichnofabrics. Characteristic bioglyphically preserved trace fossil assemblages and poorly developed bioturbational fabrics of lower–middle Cambrian (**a**–**d**), Cambro-Ordovician (**e**–**h**) and Ordovician–Silurian (**i**–**l**) heterolithic siliciclastic successions. **a**,**e**,**i**, Characteristic style of bedding for each temporal interval. **b**, *Treptichnus* (UEXP853Gu1:004). **c**, Dense assemblage of intergradational *Rusophycus* and *Cruziana* (UCR 11140/1). **d**, Lower–middle Cambrian ichnofabric, ii 2 (YPM-IP.237260). **f**, Bioglyphically preserved arthropodal scratch marks and tool marks. **g**, Dense assemblage of high-relief and bioglyphically preserved treptichnids, *Cruziana* and other shallow-tier trace fossils. **h**, Cambro-Ordovician ichnofabric, ii 2 (UCR 11135/3). **j**, Dense and bioglyphic assemblage of *Arthrophycus*. **k**, Bioglyphically preserved *Rusophycus* of nearly dm-scale diameter (YPM-IP.237261). **l**, Ordovician–Silurian ichnofabric, ii 3 (YPM-IP.237262). **b**,**c**,**f**,**g**,**j**,**k**, Hyporelief. Scale bars, 1 cm. Field photographs unless otherwise noted. Specimens from Chapel Island Formation (**a**), Torreárboles Sandstone (**b**), Pioche Formation (**c**,**d**), Beach Formation (**e**,**h**), Powers Steps Formation (**f**,**g**), Tuscarora Formation (**i**), Clinch Formation (**j**), Juniata Formation (**k**), Mifflintown Formation (**l**).

Fig. 3) and zones of ii 1 are common within individual samples and stratigraphic intervals. Moreover, ichnofabrics are typically dominated by sub-mm- to mm-scale 'microburrows' (meiofauna-scale cryptobioturbation) cast on the bases of sub-mm- to mm-scale laminae, without significant disruption to the overall laminated fabric of the rock; large, fabric-disruptive burrows are rare.

Cambro-Ordovician strata (Fig. 1e–h; see ref. 17 for further details) are also characterized by thin, coherent beds (mm- to cm-scale; mean sandstone bed thickness = 3.4 cm (Fig. 2)) separated by well-defined and commonly non-erosive junctions. Delicate (mm- to cm-scale length, sub-mm- to mm-scale width) tool marks are common. Trace fossils occur abundantly along bed junctions and are notably larger (cm-scale; up to 10 cm diameter, 30 cm length and 5.5 cm depth), on average, than those of older assemblages. Burrows are commonly preserved as horizontal casts along bed interfaces; bed-penetrative burrowing is rare. Cambro-Ordovician trace fossil assemblages are, like lower–middle Cambrian assemblages, characterized by an exceptionally high fidelity of preservation of discrete and high-relief shallowly emplaced structures; bioglyphs are common even where assemblages are dense (up to BPBI 5) or multi-generational. In spite of the density and large size of Cambro-Ordovician trace fossils, ichnofabrics are poorly developed (sample-averaged mean ii = 2.4; Fig. 3). Although Cambro-Ordovician strata rarely attain a maximum ii of 5, these more intensely disrupted zones are commonly either of limited scale (not representative of a bed or stratigraphic interval) or consist largely of sub-mm-scale cryptobioturbation or mm-scale macroburrows.

Ordovician–Silurian strata (Fig. 1i–l) are also characterized by thin (mm- to cm-scale; mean sandstone bed thickness = 3.1 cm (Fig. 2)), coherent and largely conformable beds. Ordovician–Silurian trace fossil assemblages are commonly dense (up to BPBI 4–5) and populated by large structures (maximum burrow length > 20 cm; maximum diameter = 9 cm; maximum depth = 3.5 cm) of complex morphology, recording a range of sophisticated animal–substrate interactions. Nonetheless, discrete

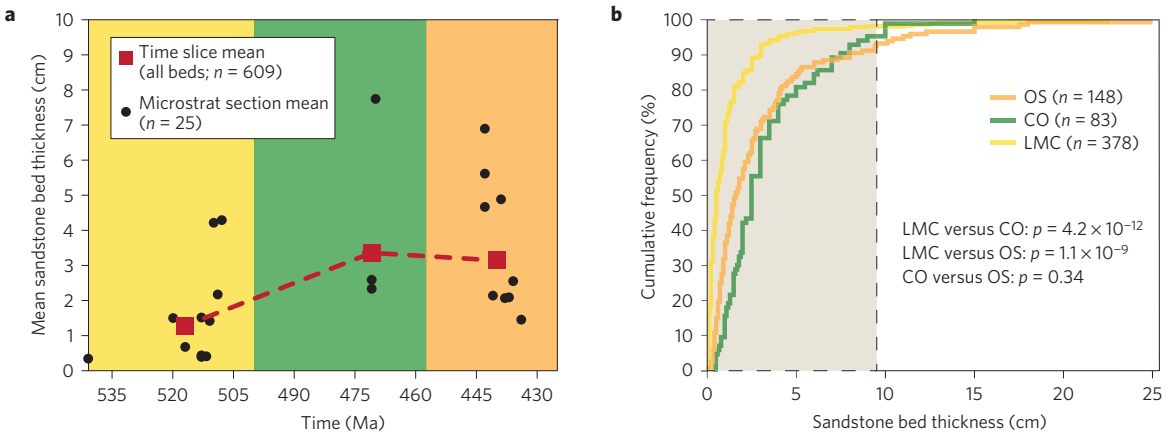

Figure 2 | Lower Palaeozoic changes in bed thickness. a,**b**, Section and time-interval averages (**a**) and cumulative frequency distributions (**b**) of individual sandstone beds, as measured in lower Palaeozoic microstratigraphic (bed-scale) sections. Binned by chronological interval: LMC, lower–middle Cambrian; CO, Cambro-Ordovician; OS, Ordovician–Silurian. The grey box in **b** denotes the extent to which this record would be erased (that is, bed junctions homogenized) by modern mean mixing intensity. *t*-test *p*-values refer to time-interval means for both **a** and **b** and denote the probability that each set of interval means is not significantly different ($p < 0.05$ denotes significant differences). Dashed lines in **a** emphasize the increase through time of mean sandstone bed thickness.

and high-relief shallowly emplaced structures are abundant; scratch marks and bioglyphic ornamentation are common, as are mm-scale tool marks. In spite of the density and large size of Ordovician–Silurian trace fossils, ichnofabrics remain poorly developed: sample-averaged mean ii = 2.8 (Fig. 3), and areas of more intensive disruption (ii 5) are spatially limited and commonly consist of sub-mm- and mm-scale disruption of individual laminae, rather than churning of entire beds or stratigraphic packages.

Lower Palaeozoic successions are, by all metrics, characterized by secular variation in mixing intensity; strata from each of the three chronological intervals are distinctly and significantly different from those of the other intervals. Trace fossil assemblages increase in density and individual trace fossils increase in size and complexity through the lower Palaeozoic. These ichnological changes are accompanied by striking changes in the stratigraphic character of bedding, particularly bed thickness (Fig. 2). The mean thickness of lower–middle Cambrian sandstone (tempestite) beds (1.3 cm) is significantly lower than those of the Cambro-Ordovician (3.4 cm) and Ordovician–Silurian (3.1 cm) (*t*-test *p*-values = 4.2×10^{-12}, 1.1×10^{-9}, respectively), reflecting a strikingly higher preponderance of thin (mm-scale) sandstone event beds than is characteristic of later intervals (Fig. 2b). The lack of these thinnest event beds in identical facies in Cambro-Ordovician and Ordovician–Silurian successions indicates that, during these later intervals, bioturbation increased sufficiently in intensity to homogenize (erase) the junctions between the thinnest event beds. Similarly, lower Palaeozoic successions are characterized by a secular increase in the intensity of fabric disruption (Fig. 3); each successive temporal interval is characterized by a mean ichnofabric index that is significantly higher than that of the preceding interval.

All stratigraphic and taphonomic metrics indicate that, in spite of secular increases in sediment colonization in general—and bioturbation in particular—through the lower Palaeozoic, sediment mixing remained limited. Average mixed layer depths, approximated as 0.2 cm, 1 cm and 1.5 cm for the early–middle Cambrian, Cambro-Ordovician and Ordovician–Silurian, respectively (see Supplementary Information), are far less than those characteristic of modern marine settings. The scale of event bedding throughout the lower Palaeozoic is far below what would survive modern intensities of sediment mixing (global mean mixed layer depth ranges from 5 to 10 cm (refs 7,8)). The anomalously high fidelity of preservation of surficial and shallowly emplaced trace fossils (Fig. 1) characteristic of these successions is anactualistic; in the majority of later Phanerozoic successions and modern marine sediments, the shallowest tiers of infaunal activity are not preserved[10]. Likewise, ii values suggest that the early Palaeozoic development of sediment mixing was an exceedingly protracted process: interval-averaged ii does not exceed 3 for any of the three intervals, and even individual samples, indicating more locally intensive but less spatially representative bioturbational events, do not attain mean ii of 5 until the lower Silurian. No ii values of 6 were observed in any of the studied successions. The coupled trace fossil and sedimentary records indicate that even 120 million years after the Precambrian–Cambrian transition, intensities of sediment mixing remained far below modern levels.

Constraints on the evolution of the global sulphur cycle can also be used to gauge the development of the mixed layer. Burrowing animals, through sediment mixing and excavation, oxygenate seafloor sediments. In modern marine environments, there is a strong correlation between mixed layer depth and the extent of sulphide reoxidation (Supplementary Fig. 2). Using a bioturbation-dependent global sulphur mass balance model[18], with previously utilized Palaeozoic sulphur cycle parameters[18–20], and our empirical estimates of mixed layer depth, we generated (see equations (1)–(3) in Methods) early Palaeozoic marine sulphate concentrations

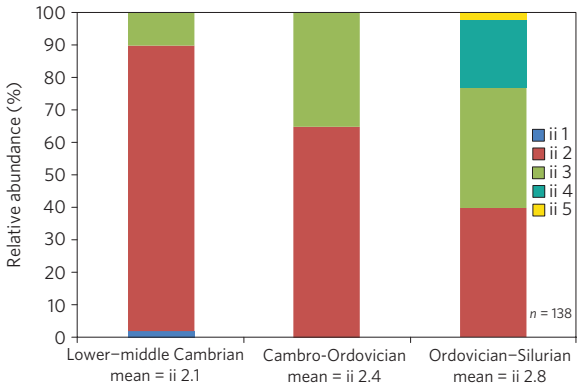

Figure 3 | Relative abundance of ichnofabric indices (ii) for each chronologic interval. *t*-test *p*-values are 0.0058 (LMC versus CO), 6.0×10^{-10} (LMC versus OS) and 0.011 (CO versus OS) and denote the probability that each set of interval means is not significantly different ($p < 0.05$ denotes significant differences).

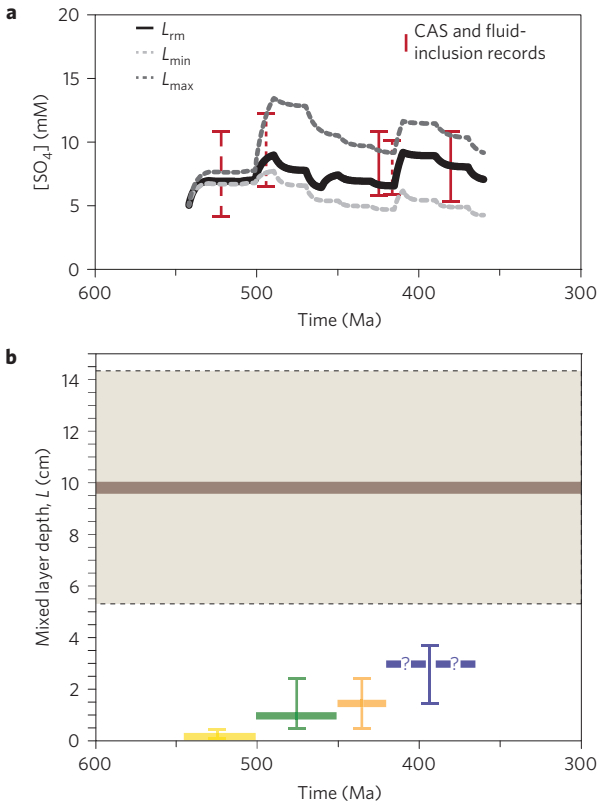

Figure 4 | Modelled results of the impact of early Palaeozoic bioturbation on contemporaneous marine sulphate concentrations [SO_4]. **a**, Model iterations were run with *x* values calculated from minimum (L_{min}; 50% predicted Devonian *L*), maximum (L_{max}; 125% predicted Devonian *L*) and preferred (L_{rm}) *L* values for each early–middle Palaeozoic interval. Model results are in close agreement with the fluid-inclusion[21,22] (solid and long-dash brackets, respectively) and modelled CAS (ref. 23) (short-dash brackets) records of this interval and indicate that bioturbation exercised a first-order control on Palaeozoic S cycling. Protracted mixed layer development resulted in near-static [SO_4] through the early Palaeozoic. **b**, Mixed layer depths derived for each early Palaeozoic interval (yellow, green and orange bands) and extrapolated for the Devonian (blue band; see Supplementary Information) are shown (with bracketed minimum and maximum estimates) in conjunction with modern mean mixed layer depth (purple band, with standard deviation denoted by dashed lines; from ref. 7).

consistent with independent geochemical records[21–23] (Fig. 4). In contrast, model simulations run with modern mixing intensities (Supplementary Figs 3a, 4 and 5) generate Cambrian–Silurian marine sulphate concentrations that are over an order of magnitude higher than independent records[21–23]. The Phanerozoic evolution of organic carbon burial would, like sulphide burial, have been strongly affected by bioturbation. A major bioturbation radiation event in the middle–late Palaeozoic (Devonian–Carboniferous) (for example, ref. 5) could, by decreasing organic carbon burial, offer an explanation for Berner's proposed mid-Devonian decline in atmospheric oxygen levels[24] (see Supplementary Information).

The exceedingly protracted development of the mixed layer suggests that bioturbation should not be viewed as the silver bullet for many of the Neoproterozoic and Cambrian geochemical, taphonomic and palaeobiological phenomena historically attributed to the development of well-mixed sediment, such as the disappearance of the Ediacara biota and declines in microbialite diversity (for example, refs 18,25–27). Even the radiation of trilobites—long considered to be largely deposit feeders, and thus sediment mixers[28,29]—does not seem to have resulted in the development of well-mixed sediments. Our constraints on the evolutionary history of sediment mixing highlight an intriguing temporal trend: advances in infaunal motility outpaced advances in sediment mixing. Infaunalization was undoubtedly well advanced by the late Silurian, as recorded by the large size, high density and architectural diversity characteristic of Silurian trace fossil assemblages. However, sediments concurrently remained poorly mixed. This decoupling of infaunalization and bioturbation implies that highly efficient sediment mixers, known as 'bulldozers' (that is, mobile deposit feeders; see ref. 5) were not yet significant members of benthic ecosystems. Presumably, the advent of widespread infaunal mobile deposit feeding was delayed by either a lack of the necessary morphological or physiological machinery or a lack of ecological pressure (for example, nutritional incentive) to exploit the mobile deposit-feeding niche. Whether morphological or ecological in cause, the protracted development of sediment mixing suggests that bulldozing made an exceedingly late-stage appearance in metazoan developmental history, and that associated restructuring of benthic ecosystems did not occur until well after both the Cambrian Explosion and the Great Ordovician Biodiversification Event.

Methods

Methods and any associated references are available in the online version of the paper.

Received 5 March 2015; accepted 17 August 2015; published online 28 September 2015

References

1. Aller, R. C. Bioturbation and remineralization of sedimentary organic-matter—effects of redox oscillation. *Chem. Geol.* **114,** 331–345 (1994).
2. Aller, R. C. in *Animal-Sediment Relations: The Biogenic Alteration of Sediments* (eds McCall, P. L. & Tevesz, M. J. S.) 53–102 (Plenum Press, 1982).
3. Aller, R. C., Yingst, J. Y. & Ullman, W. J. Comparative biogeochemistry of water in intertidal *Onuphis* (Polychaeta) and *Upogebia* (Crustacea) burrows; temporal patterns and causes. *J. Mar. Res.* **41,** 571–604 (1983).
4. Rhoads, D. C. & Young, D. K. Influence of deposit-feeding organisms on sediment stability and community trophic structure. *J. Mar. Res.* **28,** 150–178 (1970).
5. Thayer, C. W. Biological bulldozers and the evolution of marine benthic communities. *Science* **203,** 458–461 (1979).
6. Thayer, C. W. in *Biotic Interactions in Recent and Fossil Benthic Communities* (eds Tevesz, M. J. S. & McCall, P. L.) 480–595 (Plenum Press, 1983).
7. Boudreau, B. P. Mean mixed depth of sediments: The wherefore and the why. *Limnol. Oceanogr.* **43,** 524–526 (1998).
8. Teal, L. R., Bulling, M. T., Parker, E. R. & Solan, M. Global patterns of bioturbation intensity and mixed depth of marine soft sediments. *Aquat. Biol.* **2,** 207–218 (2008).
9. Teal, L. R., Parker, E. R. & Solan, M. Sediment mixed layer as a proxy for benthic ecosystem process and function. *Mar. Ecol. Prog. Ser.* **414,** 27–40 (2010).
10. Bromley, R. G. & Ekdale, A. A. Composite ichnofabrics and tiering of burrows. *Geol. Mag.* **123,** 59–65 (1986).
11. Tarhan, L. G. & Droser, M. L. Widespread delayed mixing in early to middle Cambrian marine shelfal settings. *Palaeogeogr. Palaeoclimatol. Palaeoecol.* **399,** 310–322 (2014).
12. Mangano, M. G. & Buatois, L. A. Decoupling of body-plan diversification and ecological structuring during the Ediacaran–Cambrian transition: Evolutionary and geobiological feedbacks. *Proc. R. Soc. B* **281,** 20140038 (2014).
13. Bluth, G. J. S. & Kump, L. R. Phanerozoic paleogeology. *Am. J. Sci.* **291,** 284–308 (1991).
14. Middleburg, J. J., Soetaert, K. & Herman, P. M. J. Empirical relationships for use in global diagenetic models. *Deep-Sea Res. I* **44,** 327–344 (1997).
15. Miller, M. F. & Smail, S. E.. A semiquantitative field method for evaluating bioturbation on bedding planes. *Palaios* **12,** 391–396 (1997).
16. Droser, M. L. & Bottjer, D. J. A semiquantitative field classification of ichnofabric. *J. Sediment. Petrol.* **56,** 558–559 (1986).
17. Tarhan, L. G., Droser, M. L. & Hughes, N. C. Exceptional trace fossil preservation and mixed layer development in Cambro-Ordovician siliciclastic strata. *Mem. Assoc. Australas. Palaeontol.* **45,** 71–88 (2014).
18. Canfield, D. E. & Farquhar, J. Animal evolution, bioturbation, and the sulfate concentration of the oceans. *Proc. Natl Acad. Sci. USA* **106,** 8123–8127 (2009).

19. Wu, N. P., Farquhar, J., Strauss, H., Kim, S. T. & Canfield, D. E. Evaluating the S-isotope fractionation associated with Phanerozoic pyrite burial. *Geochim. Cosmochim. Acta* **74,** 2053–2071 (2010).
20. Leavitt, W. D., Halevy, I., Bradley, A. S. & Johnston, D. T. Influence of sulfate reduction rates on the Phanerozoic sulfur isotope record. *Proc. Natl Acad. Sci. USA* **110,** 11244–11249 (2013).
21. Horita, J., Zimmermann, H. & Holland, H. D. Chemical evolution of seawater during the Phanerozoic: Implications from the record of marine evaporites. *Geochim. Cosmochim. Acta* **66,** 3733–3756 (2002).
22. Brennan, S. T., Lowenstein, T. K. & Horita, J. Seawater chemistry and the advent of biocalcification. *Geology* **32,** 473–476 (2004).
23. Gill, B. C., Lyons, T. W. & Saltzman, M. R. Parallel, high-resolution carbon and sulfur isotope records of the evolving Paleozoic marine sulfur reservoir. *Palaeogeogr. Palaeoclimatol. Palaeoecol.* **256,** 156–173 (2007).
24. Berner, R. A. Phanerozoic atmospheric oxygen: New results using the GEOCARBSULF model. *Am. J. Sci.* **309,** 603–606 (2009).
25. Laflamme, M., Darroch, S. A. F., Tweedt, S. M., Peterson, K. J. & Erwin, D. H. The end of the Ediacara biota: Extinction, biotic replacement, or Cheshire Cat? *Gondwana Res.* **23,** 558–573 (2013).
26. Awramik, S. M. Precambrian columnar stromatolite diversity—reflection of metazoan appearance. *Science* **174,** 825–827 (1971).
27. Meysman, F. J. R., Middelburg, J. J. & Heip, C. H. R. Bioturbation: A fresh look at Darwin's last idea. *Trends Ecol. Evol.* **21,** 688–695 (2006).
28. Seilacher, A. Trilobite palaeobiology and substrate relationships. *Trans. R. Soc. Edinburgh* **76,** 231–237 (1985).
29. Seilacher, A. *Trace Fossil Analysis* (Springer, 2007).

Acknowledgements

This research was supported by an NSF Graduate Research Fellowship, Amherst College John Mason Clarke Fellowship, Janet M. Boyce Memorial Fellowship and grants from the Society for Sedimentary Geology, Geological Society of America, Paleontological Society, American Museum of Natural History, Sigma Xi, InfoQuest Foundation, Evolving Earth Foundation and the Community Foundation (L.G.T.), as well as the NSF Earth-Life Transitions Program and NASA NAI UCR node (N.J.P.) and NASA NAI MIT node (D.J.T.). Permitted access to sections was provided by the Fortune Head Ecological Reserve (Canada) and Death Valley National Park (USA). Fieldwork was facilitated by D. Auerbach, E. Conrado, R. Dahl, J. Esteve, T. Garlock, J. Gehling, E. Haddad, C. Hall, L. Hancock, S. Jensen, L. Joel, T. Johnston, K. Keenan, N. McKenzie, A. Miller, P. Myrow, A. Ruiz, A. Sappenfield and R. Thomas. This paper benefited from discussion with D. Hardisty and C. Reinhard.

Author contributions

L.G.T. conceived the study, with input from all authors. L.G.T. collected all field data and performed analyses. L.G.T. and N.J.P. developed the bioturbation-dependent sulphate model, with input from D.T.J. L.G.T. wrote the manuscript with input from all authors.

Additional information

Supplementary information is available in the online version of the paper. Reprints and permissions information is available online at www.nature.com/reprints. Correspondence and requests for materials should be addressed to L.G.T.

Competing financial interests

The authors declare no competing financial interests.

Methods

Data collection and assessment of sediment mixing intensity. Bioturbation data were collected from lower Palaeozoic (lowermost Cambrian through upper Silurian) heterolithic siliciclastic shallow marine (continental margin and shelfal) successions worldwide (Supplementary Fig. 1). Stratigraphic units were selected for study on the basis of age, thickness (10 m- to 100 m-scale), continuity, exposure, lithological heterogeneity and—as determined on the basis of facies, fauna and palaeogeographic reconstructions—deposition under shallow (shelfal) oxygenated marine conditions. Siliciclastic units were selected because siliciclastic sediment and strata represent the vast majority of both the modern seafloor and the stratigraphic record (for example, ref. 13), and generally contain better-preserved and more abundant trace fossils than carbonate successions. Furthermore, lithologically heterogeneous units—thinly (mm- to dm-scale) bedded and interbedded mudstone, siltstone and sandstone—are characterized by higher stratigraphic resolution and frequency of bed-junction preservation, and therefore were selected to maximize resolution of mixing trends (see ref. 30) and correct for facies variability. Sandy heterolithic successions, moreover, undergo very limited compaction (for example, ref. 31); therefore, data collected from sand-rich successions can provide reasonable estimates for syndepositional mixed layer depths. Stratigraphic units were selected for study on the basis of age, thickness (10 m- to 100 m-scale) and continuity, exposure and lithological heterogeneity. Data were collected from 22 fine-grained, heterolithic units (Supplementary Fig. 1; see Supplementary Geologic Setting): the lowermost Cambrian Chapel Island Formation (Canada); lower Cambrian Uratanna Formation (Australia); lower Cambrian Wood Canyon Formation (western USA); lower Cambrian Torreárboles Sandstone (Spain); lower Cambrian Poleta and Harkless formations (western USA); lower to middle Cambrian Pioche Formation (and correlative Bright Angel Shale) (western USA); lower to middle Cambrian Carrara Formation (western USA); Cambro-Ordovician Beach Formation (Canada); Cambro-Ordovician Bynguano Formation (Australia); Lower to Middle Ordovician Wabana Group (Powers Steps, Scotia and Grebes Nest Point formations) (Canada); Upper Ordovician Juniata Formation (eastern USA); Lower Silurian Tuscarora, Rose Hill, Clinch and Rockwood formations (eastern USA); Lower to Upper Silurian Mifflintown and Red Mountain formations (eastern USA); Middle Silurian Herkimer Formation (eastern USA) and Middle to Upper Silurian Bloomsburg Formation (eastern USA).

For each stratigraphic section, data were collected at the sub-metre-scale from each one-metre-thick interval and, additionally, for facies-representative intervals of each section, from continuously sampled individual, discrete beds. Data were collected according to a number of sedimentological, ichnological and taphonomic criteria, to determine the extent of biogenic sediment mixing in typical early Palaeozoic marine shelfal environments.

Six criteria were used to characterize lower Palaeozoic strata: bedding thickness; depth of bioturbation; biogenic fabric disruption (that is, Ichnofabric Index); fidelity of trace fossil preservation (that is, bioglyphic preservation); palaeobiological and palaeoecological complexity of trace fossil assemblages and abundance of surficially produced physical sedimentary structures.

Bedding thickness: The thickness of beds separated by clear bed junctions indicates the maximum depth to which bioturbation penetrated without having disrupted the coherency of individual beds. Bedding thickness was assessed on the individual bed scale (absolute thickness, measured for each individual, discrete bed) over representative, 50 cm- or 100 cm-thick 'microstratigraphic sections.' Furthermore, bedding thickness was assessed on the package scale (approximate thickness of beds, demarcated as mm-scale [1–10 mm], cm-scale [1–10 cm], dm-scale [1–10 dm] or m-scale [≥1 m], determined for individual lithologically distinct facies packages over each one-metre stratigraphic interval) for each stratigraphic section (tens to hundreds of metres).

Fabric disruption: The ichnofabric index (ii) of Droser and Bottjer[16] schematically demarcates the intensity of infaunal disruption of sedimentary fabrics (that is, extent of preservation of primary physical sedimentary structures) into six indices, ranging from ii 1 (laminated) to ii 2 (discrete but isolated burrows, up to 10% of depositional fabric disrupted), ii 3 (both isolated and locally overlapping burrows, approximately 10-40% of depositional fabric disrupted), ii 4 (last vestiges of depositional fabric preserved, approximately 40–60% of depositional fabric disrupted), ii 5 (no vestige of depositional fabric, but discrete burrows still visible) and ii 6 (completely homogenized—neither depositional fabric nor discrete burrows are preserved). Ichnofabric index was measured throughout field exposures, wherever possible, as well as for selected hand samples (100 cm^3- to 1,000 cm^3-scale), which were collected at regular (m-scale or finer) intervals from each distinct facies package, cut, polished and scanned. For each hand sample, maximum ichnofabric index (irrespective of scale) and average ('whole-rock') ichnofabric index were measured. Average ichnofabric indices were measured to provide scale normalization (for example, a 1 cm^2 zone of ii 6, although a valid maximum ichnofabric index, is not necessarily representative of a bed or stratigraphic interval). In this regard, maximum ichnofabric indices are illustrative as to infaunal behaviour, whereas average ('whole-rock') ichnofabric indices are better metrics of the extent of sediment mixing. Subsequently, the mean of individual sample-averaged ichnofabric index measurements was calculated for each time interval to measure shifts in the range of variability characteristic of each time interval.

Depth of bioturbation: The depth of discrete burrows, where contact with the ancient sediment–water interface can be clearly determined, indicates the maximum depth of the zone of infaunal activity (that is, the infaunal 'habitable zone'). This, in turn, provides information concerning the morphological and physiological ability of animals to penetrate the substrate. Maximum burrow depth was noted, wherever possible, over each stratigraphic interval.

Bioglyphic preservation: The presence of bioglyphs—finely-preserved burrow ornamentation or other organismal 'fingerprints' such as arthropod scratch marks or appendage imprints[32]—was employed as an indicator of exceptional preservation and thus a firm (that is, unmixed) substrate at the depth of emplacement. The presence or absence of bioglyphic preservation was noted throughout all measured stratigraphic successions.

Palaeobiological and palaeoecological complexity: The morphological and assemblage-level complexity of shallowly emplaced trace fossils, including trace fossil size, density, diversity, architectural complexity and taphonomy was noted throughout each stratigraphic section as a metric of the extent and character of substrate colonization. Trace fossil morphology and ichnogeneric diversity were noted. Ichnotaxa were characterized as 'abundant,' 'common' or 'rare', according to how frequently they were observed; for example, for a given stratigraphic metre: present on each bedding plane or multiple occurrences per bedding plane ('abundant'); multiple occurrences within 1 m ('common') or <5 occurrences per metre ('present' or 'rare'). The occurrence of complete open burrows, such as *Treptichnus*, *Gyrolithes*, *Monocraterion* (for example, refs 33–35) was used as a metric for preservation of the palaeo-sediment–water interface, whereas truncated burrows and infill by foreign material indicated intensive and multi-generational substrate colonization and sediment mobilization[10]. In addition, the bedding plane bioturbation index (BPBI) of Miller and Smail[15], which demarcates burrowed bed surfaces according to the density of surface coverage and disruption (from BPBI 1 [0% disruption] to BPBI 5 [60–100% disruption]), was used to characterize the extent of infaunal colonization of bedding plane exposures. Cross-cutting and consistent tiering relationships were further used to quantify maximum depth of bioturbation[10,36].

Surficially produced physical sedimentary structures: All observed surficially produced physical sedimentary structures, such as scratch circles, tool marks and flute marks, which require hydroplastic or cohesive sediment to form and be preserved[37], were noted. Further, for all available basal bedding plane exposures, the occurrence of tool marks and similar features was quantified as 'absent,' 'present/rare,' 'common' or 'abundant' (according to the same metrics as those used to quantify trace fossil assemblages).

Specimens reposited in the Invertebrate Paleontology collections of the Yale Peabody Museum (YPM) and University of California, Riverside (UCR) and the collections of the Área de Paleontología, Universidad de Extremadura (UEX).

Model description. The model we employ builds from a previously developed bioturbation-dependent global sulphur mass balance model[18]. Using this model, marine sulphate concentrations will vary as a response to marine sulphur burial fluxes:

$$\frac{d[SO_4]}{dt} = Flux_{in} - Flux_{out} \quad (1)$$

where $[SO_4]$ is the sulphate concentration of the global ocean at a given time t, $Flux_{in}$ is the sulphur input flux, and where $Flux_{out}$, the sulphur output flux, can be expressed by:

$$Flux_{out} = \frac{x SR_{t-1}}{f_{pyr}} \quad (2)$$

where x is the stoichiometric proportion of sulphide that escapes reoxidation, f_{pyr} is the proportion of sulphur buried as pyrite and SR is the globally integrated sulphate reduction rate. We solved this equation using the Euler method and a time-step of 300,000 years. We utilized f_{pyr} values for the early and middle Palaeozoic derived from the stratigraphic record of previously reported $\delta^{34}S_{sulphide}$ and $\delta^{34}S_{sulphate}$ values (Supplementary Table 2) and exploring a range of input flux parameters (see refs 18–20,38,39). Data from a range of modern marine localities (Supplementary Table 3) indicate that mixed layer depth (L) and x have a strong exponential correlation (Supplementary Fig. 2; $r^2 = 0.91$):

$$x = 0.84183e^{-0.25L} \quad (3)$$

This modern relationship was used to calculate Palaeozoic x values, using Palaeozoic L values derived from the suite of mixing intensity data discussed above (see Supplementary Information (for example, Supplementary Table 1) for full model derivation and parameter values). We explored the sensitivity of the model to variation in the magnitude of the sulphur input flux ($Flux_{in}$), isotopic value of the input flux ($\delta^{34}S_{in}$), f_{pyr}, organic carbon availability and the exponential scaling

between sulphate reduction rate (SR) and [SO_4]; the relationship between modern x and L; and modern versus Palaeozoic L. Within the parameter space explored, the model was by far most sensitive to the extent of bioturbation (L values). These sensitivity tests are presented in Supplementary Figs 3–5.

References

30. Crimes, T. P. Production and preservation of trilobite resting and furrowing traces. *Lethaia* **8,** 35–48 (1975).
31. Berner, R. A. *Early Diagenesis: A Theoretical Approach* (ed. Holland, H. D.) (Princeton Series in Geochemistry, Princeton Univ. Press, 1980).
32. Ekdale, A. A. & De Gibert, J. M. Paleoethologic significance of bioglyphs: Fingerprints of the subterraneans. *Palaios* **25,** 540–545 (2010).
33. Droser, M. L., Jensen, S., Gehling, J. G., Myrow, P. M. & Narbonne, G. M. Lowermost Cambrian ichnofabrics from the Chapel Island Formation, Newfoundland: Implications for Cambrian substrates. *Palaios* **17,** 3–15 (2002).
34. Jensen, S., Saylor, B. Z., Gehling, J. G. & Germs, G. J. B. Complex trace fossils from the terminal Proterozoic of Namibia. *Geology* **28,** 143–146 (2000).
35. Vannier, J., Calandra, I., Gaillard, C. & Zylinska, A. Priapulid worms: Pioneer horizontal burrowers at the Precambrian–Cambrian boundary. *Geology* **38,** 711–714 (2010).
36. Wetzel, A. & Aigner, T. Stratigraphic completeness: Tiered trace fossils provide a measuring stick. *Geology* **14,** 234–237 (1986).
37. Elliott, R. E. A classification of subaqueous sedimentary structures based on rheological and kinematical parameters. *Sedimentology* **5,** 193–209 (1965).
38. Halevy, I., Peters, S. E. & Fischer, W. W. Sulfate burial constraints on the Phanerozoic sulfur cycle. *Science* **337,** 331–334 (2012).
39. Canfield, D. E. Sulfur isotopes in coal constrain the evolution of the Phanerozoic sulfur cycle. *Proc. Natl Acad. Sci. USA* **110,** 8443–8446 (2013).